Combined Fictitious Sources - Scattering Matrix method

Gérard Tayeb, Stefan Enoch

Combined Fictitious Sources - Scattering Matrix method

Gérard Tayeb, Stefan Enoch

Institut Fresnel, UMR CNRS 6133,

Faculté des Sciences et Techniques de Saint-Jérôme, Case 161

13397 Marseille Cedex 20, France

e-mail: gerard.tayeb@fresnel.fr ; stefan.enoch@fresnel.fr

Abstract:

This paper describes a way to combine the method of fictitious sources and the scattering matrix method. The resulting method holds concurrently the advantages of these two rigorous methods. It is able to solve efficiently electromagnetic problems where the structure is made of a jacket containing an arbitrary set of scatterers. The method is described in a two-dimensional case, but the basic ideas could be easily extended to three-dimensional cases.

OCIS codes:

050.1960 Diffraction theory

260.2110 Electromagnetic theory

1. Introduction

The scattering matrix method (SMM) [1] applies to the scattering of a finite set of parallel cylinders of arbitrary cross-sections and arbitrary electromagnetic constants placed in a single homogeneous medium. It is based on the expansion of the fields in terms of Fourier-Bessel series around each cylinder. Using the scattering matrices of each cylinder and the translation properties of Fourier-Bessel functions, the method leads to the inversion of a linear set of equations. The method is rigorous and very efficient. It can deal for instance with photonic crystals (with or without defects) made of several hundreds of cylinders on a standard personal computer.

On the other hand, the SMM is not able to deal with some interesting configurations, specially when the set of cylinders is surrounded by a jacket. In the case of a jacket with circular cross-section, it is possible to extend the SMM by expanding the field around the jacket using again Fourier-Bessel series.[2] This idea has also been implemented for the study of microstructured optical fibers.[3]

In this paper, we extend the method to the case of a jacket with arbitrary cross-section. For that purpose, we combine the SMM with the method of Fictitious Sources (MFS).

The MFS method [4] is able to solve the problem of scattering from arbitrary scatterers. In this method, the space is divided in different regions where the field is represented as the field radiated by a set of fictitious sources with unknown intensities. These intensities are obtained by matching the fields at the boundaries of the regions using a least squares technique.

The basic idea of the method proposed in this paper is to use the SMM in order to build a set of functions that correctly represent the field inside the jacket. These functions are then used to solve a fictitious sources problem on the boundary of the jacket.

With this combined use of the SMM and MFS methods, we hold concurrently the advantages of these two rigorous methods, and can address efficiently new classes of problems, such as a finite dielectric body drilled by galleries, that can be for instance a macroporous silicon crystal.

The problem under study and our notations are described in section 2. In sections 3 and 4, we recall the basis of the MFS and the SMM. Section 5 describes the combined use of these two methods, and section 6 provides some numerical illustrations of the resulting method.

2. Setting of the problem

Through the whole paper, we use an orthogonal coordinate system with unit vectors $\hat{\mathbf{x}}, \hat{\mathbf{y}}, \hat{\mathbf{z}}$. We consider time-harmonic problems, and the fields are represented by complex quantities using a time dependence in $\exp(-i\omega t)$. We denote by ε_0 and μ_0 the permittivity and the permeability of vacuum, and by $k_0 = 2\pi/\lambda_0 = \omega(\varepsilon_0\mu_0)^{1/2}$ the wave number. For simplicity, we assume that all the media have the permeability μ_0, but the principle of the method would remain unchanged if it were not the case. We consider a two-dimensional problem, assuming that the entire structure is invariant along the *z* axis (Fig. 1). The cylindrical scatterer is limited by its external boundary $\mathscr{C}_0$. The exterior of $\mathscr{C}_0$ is the domain Ω_e, filled with a medium with optical index n_e (n_e may be complex, and we note $k_e = k_0\, n_e$). The interior of $\mathscr{C}_0$ is the domain Ω_i. It is filled with a medium with optical index n_i (grayed region in Fig. 1; n_i may be complex, and we put $k_i = k_0\, n_i$), but also contains cylindrical rods with boundaries $\mathscr{C}_j$ (j = 1, 2, 3,…), filled with arbitrary media.

The structure is illuminated by an incident field coming from the exterior (this assumption is made for clarity, but the method can also deal with an excitation from inside $\mathscr{C}_0$ with very little modification). This incident field is also assumed to be *z*-independent. For instance, it can be a plane wave, or the field emitted by one (or several) line source(s) placed outside $\mathscr{C}_0$. It is well known that in that case the problem can be reduced to two independent problems: the *s* polarization case where the electric field is parallel to the *z* axis, and the *p* polarization case where the magnetic field is parallel to the *z* axis. Each of these cases leads to a scalar problem where the unknown u is the z component of either **E** or **H**: $u = E_z$ (in *s* polarization) or $u = H_z$ (in *p* polarization). We denote by u^{inc} the incident field, and by u^{scat} the scattered field, in such a way that the total field is:

$$\begin{cases} u = u^{inc} + u^{scat} & \text{in } \Omega_e \text{ (outside } \mathscr{C}_0) \\ u = u^{int} & \text{in } \Omega_i \text{ (inside } \mathscr{C}_0) \end{cases} . \tag{1}$$

3. The Method of Fictitious Sources (MFS)

The MFS is a versatile and reliable method able to deal with many scattering problems. It relies upon a simple idea: the electromagnetic field in the various domains of the diffracting structure is expressed as a combination of fields radiated by adequate electromagnetic sources. These sources have no physical existence, and this is why we have called them "fictitious" sources. They are located in homogeneous regions, and not on the interfaces. In other words, one can consider that they generate electromagnetic fields that faithfully map the actual field, thus they form a convenient basis for this field. From a numerical point of view, proper bases are those capable of representing the solution with the fewest number of functions. Obviously, the quality

of the bases is closely linked with the nature of the sources and their location. The freedom in the choice of the sources provides a great adaptability to various complex problems.

The MFS has been developed in our Laboratory in the last decade, both from theoretical and numerical points of view.[4-8] Almost at the same time and independently, some other groups have worked on the same basic ideas,[9-14] but their approaches are slightly different from ours. In fact, one of the first attempt at using this method is probably due to Kupradze.[15] The method has been developed and applied to a large collection of problems, and a good review can be found in Ref. [16]. It is not our goal to depict here all the details of the MFS, and it will be sufficient for our purpose to give an outline of the general principle.

Let us consider the same situation as in Figure 1, but without the inclusions: the interior region Ω_i is thus filled with an homogeneous material with optical index n_i (Fig. 2). Let us imagine a set of N fictitious sources $S_{e,n}$ ($n = 1,2,\ldots,N$) located at N points $\mathbf{r}_{e,n}$ in Ω_i, and supposed to radiate in free space filled with a medium with the index n_e. Let us denote by $F_{e,n}(\mathbf{r})$ the field radiated by the source $S_{e,n}$. By construction, the fields $F_{e,n}(\mathbf{r})$ satisfy the Maxwell's equations in Ω_e, and a radiation condition at infinity. A linear combination $\sum_n c_{e,n} F_{e,n}(\mathbf{r})$ can thus be regarded as an approximation $\tilde{u}^{scat}(\mathbf{r})$ of the diffracted field $u^{scat}(\mathbf{r})$ in Ω_e, where $c_{e,n}$ can be understood as the complex amplitude of the source $S_{e,n}$. So we obtain an approximation for the field in Ω_e:

$$\tilde{u}^{scat}(\mathbf{r}) \overset{def}{=} \sum_{n=1}^{N} c_{e,n} F_{e,n}(\mathbf{r}) \ , \text{ in } \Omega_e , \tag{2}$$

and thus:

$$u(\mathbf{r}) \approx u^{inc}(\mathbf{r}) + \sum_{n=1}^{N} c_{e,n}\, F_{e,n}(\mathbf{r}) \ , \text{ in } \Omega_e \,, \tag{3}$$

In the same way, we imagine another set of fictitious sources $S_{i,n}$ (n = 1,2,…,N) located at N points $\mathbf{r}_{i,n}$ in Ω_e, and supposed to radiate in free space filled with a medium with the index n_i. Let us denote by $F_{i,n}(\mathbf{r})$ the field radiated by the source $S_{i,n}$. The functions $F_{i,n}(\mathbf{r})$ verify the Maxwell's equations in Ω_i, and can be used to get an approximate expansion $\tilde{u}^{int}(\mathbf{r})$ of the total field $u^{int}(\mathbf{r})$ in Ω_i:

$$\tilde{u}^{int}(\mathbf{r}) \overset{def}{=} \sum_{n=1}^{N} c_{i,n}\, F_{i,n}(\mathbf{r}) \ , \text{ in } \Omega_i \,, \tag{4}$$

where $c_{i,n}$ can be understood as the complex amplitude of the source $S_{i,n}$.

Note that the nature of the sources can be chosen arbitrarily. In our case, we choose infinitely thin line sources parallel to the z axis: $S_{e,n}(\mathbf{r}) = 4i\ \delta(\mathbf{r} - \mathbf{r}_{e,n})$ and $S_{i,n}(\mathbf{r}) = 4i\ \delta(\mathbf{r} - \mathbf{r}_{i,n})$. In that case, they radiate the fields:

$$F_{e,n}(\mathbf{r}) = \mathrm{H}_0^{(1)}\left(k_e \left|\mathbf{r} - \mathbf{r}_{e,n}\right|\right), \tag{5}$$

$$F_{i,n}(\mathbf{r}) = \mathrm{H}_0^{(1)}\left(k_i \left|\mathbf{r} - \mathbf{r}_{i,n}\right|\right). \tag{6}$$

The determination of the coefficients $c_{e,n}$ and $c_{i,n}$ is obtained by matching the boundary conditions on the cylinder surface $\mathscr{C}_0$. For a given function $\varphi(\mathbf{r})$, let us denote by $D\varphi(\mathbf{r})$ the value of its normal derivative on $\mathscr{C}_0$. The exact solution verifies

$$\begin{cases} u^{inc}(\mathbf{r}) + u^{scat}(\mathbf{r}) - u^{int}(\mathbf{r}) = 0 & \text{on } \mathscr{C}_0 \\ Du^{inc}(\mathbf{r}) + Du^{scat}(\mathbf{r}) - p\, Du^{int}(\mathbf{r}) = 0 & \text{on } \mathscr{C}_0 \end{cases}, \tag{7}$$

where p is a polarization dependent constant equal to

$$\begin{cases} p = 1 & \text{in } s \text{ polarization case} \\ p = (n_e / n_i)^2 & \text{in } p \text{ polarization case} \end{cases}. \tag{8}$$

The coefficients $c_{e,n}$ and $c_{i,n}$ that give the better approximation for the fields (2) and (4) are those that match the boundary conditions in the best way. They are obtained by minimizing the two expressions derived from (7) and defined on $\mathscr{C}_0$:

$$\begin{cases} u^{inc}(\mathbf{r}) + \sum_{n=1}^{N} c_{e,n}\, F_{e,n}(\mathbf{r}) - \sum_{n=1}^{N} c_{i,n}\, F_{i,n}(\mathbf{r}) \\ Du^{inc}(\mathbf{r}) + \sum_{n=1}^{N} c_{e,n}\, DF_{e,n}(\mathbf{r}) - p \sum_{n=1}^{N} c_{i,n}\, DF_{i,n}(\mathbf{r}) \end{cases}. \tag{9}$$

This can be done by several ways. The simplest one is to use a point matching method that enforces the vanishing of these two expressions on sample points on $\mathscr{C}_0$. By this way, we can get a system of $2N$ equations for the $2N$ unknowns $c_{e,n}$ and $c_{i,n}$. From our numerical experiments, it emerges that it is preferable to use an overdetermined system and to solve it in the least-squares sense.[17] By this way, and for a given computation time, we obtain a better approximation for u^{scat} and u^{int}.

Of course, the efficiency of the method depends on the location and the number N of the fictitious sources. It can be shown that the precision of the method is related to the least-squares

remainder obtained in the last step, which thus can be used to quantize the quality of the solution. This feature is quite helpful in the numerical implementation.

The interested reader will find more details in Ref. [4]. We have also developed some tricks in order to place the sources automatically. The general idea used in these tricks is to increase the number of sources where the radius of curvature of $\mathscr{C}_0$ is lower. An example is given in Fig. 3. The cross-section of the cylinder $\mathscr{C}_0$ mimics a rounded F letter (first letter of Fresnel Institute), and it is given by a parametric equation

$$z(t) = x(t) + i\ y(t) = \sum_{n=-5,5} c_n \exp(in2\pi t)\,. \tag{10}$$

The values of the coefficients c_n are given in the Fig. 3 caption. We use N = 200 sources in each region Ω_e and Ω_i, and 2N sample points on $\mathscr{C}_0$. This cylinder of index $n_i = 1.5$ lies in vacuum ($n_e = 1$) and is illuminated with an incidence $\theta^{inc} = -45°$ by a plane wave with wavelength $\lambda_0 = 2$ and unit amplitude. Figure 4 gives the intensity $D(\theta)$ scattered at infinity in the direction θ. It is defined in the following way: due to the asymptotic behavior of the Hankel function, the scattered field at infinity writes (with $r = |\mathbf{r}|$) :

$$u^{scat}(\mathbf{r}) \approx g(\theta)\,\frac{\exp(ik_e r)}{\sqrt{r}}\ , \tag{11}$$

and the intensity scattered at infinity is

$$D(\theta) = 2\pi\left|g(\theta)\right|^2\ . \tag{12}$$

Finally, Fig. 5 shows the field map in the vicinity of the scatterer.

4. The Scattering Matrix Method (SMM)

This method is able to solve the problem of the diffraction by an arbitrary set of parallel cylinders placed in a homogeneous medium. A detailed description can be found in Ref. [1]. Note that the method is also called "multipole method" by other authors and has been used to study the local density of states in photonic crystals,[18] as well as microstructured optical fibers.[3] We only give below an outline of the basic ideas.

We consider a set of N_c parallel cylinders $\mathscr{C}_j$, as shown in Fig. 6. In order to lay the ground for the next section, we assume that the medium outside the cylinders has the index n_i defined in section 2. The incident field u^{inc} can be arbitrary (plane wave, line source,…).

For any cylinder $\mathscr{C}_j$, we consider a circle $\mathscr{D}_j$ with center O_j, in such a way that the cylinder is completely inside $\mathscr{D}_j$ (Fig. 7). Due to the properties of the Helmholtz equation, the total field $u(P)$ at a point P on $\mathscr{D}_j$ can be written as a "Fourier-Bessel" expansion. Denoting by $r_j(P)$ and $\theta_j(P)$ the polar co-ordinates in the local system (O_j, x_j, y_j), we can write:

$$u(P) = \sum_{m=-\infty,+\infty} \left[a_{j,m}\, J_m(k_i\, r_j(P)) + b_{j,m}\, H_m^{(1)}(k_i\, r_j(P)) \right] \exp(i\, m\, \theta_j(P)) \ . \qquad (13)$$

The two terms in the preceding series (13) can be interpreted in the following way. The second term satisfies a radiation condition and thus represents the field scattered by the cylinder $\mathscr{C}_j$. For each cylinder, this scattered field will be characterized by the matrix column $\mathbf{b}_j$ containing the $b_{j,m}$ elements. The first term represents the local incident field on the cylinder $\mathscr{C}_j$, generated by

the actual incident field u^{inc} as well as by the fields scattered by all the other cylinders $\mathscr{C}_k$ with $k \neq j$.

Denoting by $\mathbf{a}_j$ the matrix column containing the $a_{j,m}$, and using translation properties of Bessel functions (Graf's formula [19]), it can be obtained [1] for any cylinder $\mathscr{C}_j$ a linear relationship:

$$\mathbf{a}_j = \mathbf{Q}_j + \sum_{k \neq j} \mathbf{T}_{j,k}\, \mathbf{b}_k \ , \tag{14}$$

where $\mathbf{Q}_j$ is a known column matrix which represents the actual incident field on the cylinder $\mathscr{C}_j$, and $\mathbf{T}_{j,k}$ is a known square matrix (its elements simply contain exponentials and Hankel functions).

For any cylinder $\mathscr{C}_j$, another relation between $\mathbf{b}_j$ and $\mathbf{a}_j$ is provided by the scattering matrix $\mathbf{S}_j$ of the cylinder. The diffracted field is linked to the local incident field by:

$$\mathbf{b}_j = \mathbf{S}_j\, \mathbf{a}_j \ . \tag{15}$$

Eliminating $\mathbf{a}_j$ from (14) and (15), then collecting the equations written for each cylinder, leads to a linear system which gives the solution $\mathbf{b}_j$:

$$\begin{bmatrix} \mathbf{I} & -\mathbf{S}_1\mathbf{T}_{1,2} & \cdots & -\mathbf{S}_1\mathbf{T}_{1,N} \\ -\mathbf{S}_2\mathbf{T}_{2,1} & \mathbf{I} & ... & -\mathbf{S}_2\mathbf{T}_{2,N} \\ \vdots & \vdots & \ddots & \vdots \\ -\mathbf{S}_N\mathbf{T}_{N,1} & -\mathbf{S}_N\mathbf{T}_{N,2} & \cdots & \mathbf{I} \end{bmatrix} \begin{bmatrix} \mathbf{b}_1 \\ \mathbf{b}_2 \\ \vdots \\ \mathbf{b}_N \end{bmatrix} = \begin{bmatrix} \mathbf{S}_1\,\mathbf{Q}_1 \\ \mathbf{S}_2\,\mathbf{Q}_2 \\ \vdots \\ \mathbf{S}_N\,\mathbf{Q}_N \end{bmatrix}, \tag{16}$$

where I denotes the identity matrix. For brevity, this equation will be written as:

$$\mathbf{S}^{-1}\,\mathbf{B} = \mathbf{A}\ , \tag{17}$$

and formally inverted as:

$$\mathbf{B} = \mathbf{S}\,\mathbf{A}\ . \tag{18}$$

Now let us point out some features of the method.

1. In Eq. (18), column **A** linearly depends on the actual incident field u^{inc}, and column **B** contains the information on the field diffracted by the entire set of cylinders. In that sense, **S** is the scattering matrix of the set of cylinders. From Eq.(16), it appears that $\mathbf{S}^{-1}$ is simply built as soon as the scattering matrices $\mathbf{S}_j$ of all cylinders are known. This feature is interesting from a numerical point of view. It means that the individual scattering matrices $\mathbf{S}_j$ can be constructed independently from the main code dealing with the set of cylinders. That is the reason why we call this method Scattering Matrix Method (SMM). When the cylinders are circular, matrices $\mathbf{S}_j$ are very simple and reduce to diagonal matrices whose elements can be expressed in closed form. When the cylinders are not circular, we use an external integral code in order to compute the $\mathbf{S}_j$. Another important point is that, when all the cylinders in the set are identical, all the matrices $\mathbf{S}_j$ are also identical (because they are defined in the local co-ordinate system centered on each cylinder).

2. Solving system (16) gives the $b_{j,m}$. From that knowledge, the total field *u* is given outside the circles $\mathscr{D}_j$ by:

$$u(P) = u^{inc}(P) + \sum_{j=1}^{N_c} \sum_{m=-\infty}^{+\infty} b_{j,m}\, H_m^{(1)}(k_i\, r_j(P))\ \exp(i\, m\, \theta_j(P))\ . \tag{19}$$

The consequence is that everywhere outside the circles $\mathscr{D}_j$, the field u and also its derivatives are known in closed form by (19) and its derivatives.

3. For numerical purpose, it is clear that the series in Eq. (13) has to be truncated. It can be shown that, due to properties of the Helmholtz equation, the terms of the series are decreasing extremely fast after a given threshold is reached. Assuming that we keep M terms in the series, columns $\mathbf{a}_j$ and $\mathbf{b}_j$ reduce to M elements, matrices $\mathbf{S}_j$ have a rank M, and the linear system (16) has a rank $N_c \times M$. In fact, the value of M is closely linked with the radius ρ of the cylinders (or of $\mathscr{D}_j$ for non circular cylinders) and the wavelength $\lambda_i = 2\pi / k_i$. A convenient value for M is given by the empirical rule $M \approx 40\,\rho / \lambda_i$ (taking for M an odd integer). With such value of M, the accuracy is better than 1%. As an example, for typical values used in photonic crystals problems, we generally take $M = 7$. It means that for N = 100 cylinders, we solve a 700 by 700 system.

4. The incident field is arbitrary. It can be a plane wave, a Gaussian beam, or the field emitted by one (or several) infinitely thin line source parallel to the z axis, acting as an antenna. For the purpose of this paper, we are mainly interested by this last case, and u^{inc} is then given by expressions similar to Eq. (6). Note that the incident field only appears in the second member of (16), and consequently dealing with several incident fields is numerically very efficient.

5. Last, we must point out one limitation of the method. The Fourier-Bessel expansion in Eq. (13) is valid only if the circle $\mathscr{D}_j$ lies in an homogeneous medium. It means that the circle which contains one cylinder cannot intersect the boundary of another cylinder. In other words, one can remind that the circles $\mathscr{D}_j$ must have no intersection. Of course, it is always so when the cylinders are circular. In fact, for non-circular cylinders, the problem is much more subtle, and

the method should also work in some cases where the circles intersect. The problem is similar to the problem of validity of the "Rayleigh hypothesis" in grating theory.[20]

5. Hybrid method using MFS and SMM

Let us come back to the original problem described in section 2. This problem can be solved by a slight modification of the method of fictitious sources described in section 3.

Indeed, the scattered field can be still expressed as in Eq. (2), using the same fictitious sources $S_{e,n}$ (line sources that radiate $F_{e,n}(\mathbf{r})$ fields expressed as Hankel functions exactly as in Eq. (5)).

But in that case, the $F_{i,n}(\mathbf{r})$ functions used to expand the field in Ω_i (inside $\mathscr{C}_0$) must be changed. Let us consider the problem depicted in Fig. 8. The inclusions $\mathscr{C}_j$ are immersed in a medium with index n_i (the boundary $\mathscr{C}_0$ of the external scatterer is suppressed). We keep the same line sources $S_{i,n}$ as in section 3. The new $F_{i,n}(\mathbf{r})$ function is the total field when the structure of Fig. 8 is excited by the source $S_{i,n}$. By solving this problem as proposed in section 4, $F_{i,n}(\mathbf{r})$ can be expressed by the expansion (19). In other words, $F_{i,n}(\mathbf{r})$ ($n=1,2,...,N$) is a set of solutions for the total field inside $\mathscr{C}_0$, that are available in closed form, and that can be used to expand the field in Ω_i following Eq. (4). Using (19), we can compute the value of $F_{i,n}(\mathbf{r})$ and its normal derivative on $\mathscr{C}_0$, and get the expressions (9) to be minimized. This minimization gives the coefficients $c_{e,n}$ and $c_{i,n}$, and we finally get the expressions of the total field in closed form everywhere using (3) in Ω_e and (4) in Ω_i.

6. Numerical examples

We begin by a comparison with the a result of Ref. [2]. With the notations of section 2, $\mathscr{C}_0$ is a circle with radius 10 (arbitrary units), the outside medium is vacuum ($n_e = 1$), and $n_i = 4$. The inclusions are circular cylinders filled with vacuum, with radius 0.8, and arranged with a hexagonal symmetry, with the distance between the centers of the cylinders equal to 4. The central cylinder is suppressed. The structure is illuminated with a plane wave in *p* polarization case, coming from the top of the figure, with an amplitude normalized to unity. The wavelength $\lambda_0 = 22$ is chosen in order to get a resonant localized mode inside the structure. Figure 9 shows the modulus of the total field. It is quite similar to the Fig. 7 of Ref. [2], except inside the small cylinders, where we are inclined to trust in our computation. Note that the method described in Ref. [2] can only deal with an external boundary $\mathscr{C}_0$ with a circular shape.

In a second example, we illustrate some possibilities of the method on a more complex situation. As in section 3, the cross-section of the cylinder $\mathscr{C}_0$ is a F letter, but now with sharp edges. The reason of this choice is only to prove that the method also works pretty well in that case, which is more difficult to solve than a cylinder with rounded boundaries. All the coordinates of $\mathscr{C}_0$ corners in the (*x*,*y*) plane have integer values that can be deduced from Fig. 10. The profile $\mathscr{C}_0$ is described by a series identical to Eq.(10), but in this case we use a large number of c_n coefficients ($n = -100,100$) in order to get a quasi polygonal shape. For the interested reader, some more details on the technical parameters relative to the computations are available.[21] This scatterer of index $n_i = 1.5$ lies in vacuum ($n_e = 1$). There are also four inclusions inside $\mathscr{C}_0$. The elliptical one has principal axes with half dimensions equal to 1 and

0.5, its center is in (-1,4), its principal axes are rotated 45° apart from the (*x*,*y*) axes, and it is made of infinitely conducting material. The rectangular one is placed in the region $-1.5 < x < -0.5$ and $-2 < y < 0$, and is filled with vacuum. One of the circular inclusions has its center in (2,-1), a radius of 0.5, and it is filled with vacuum. The second circular inclusion has its center in (3,4), a radius of 0.5, and it is filled with a lossy material with optical index $0.5 + 2i$ (typical value for a metal in the optical range). This structure is illuminated with an incidence $\theta^{inc} = -45°$ by a plane wave with wavelength $\lambda_0 = 2$ and *p* polarization. In that case, the number of sources in each region Ω_e and Ω_i is taken to $N = 500$. The total H_z field map is shown in Fig. 10. Note that the present version of our numerical code do not allow to compute the field inside a circle which includes elliptical or rectangular bodies. It is the reason why dark areas appear around these two inclusions.

Our last and more practical example illustrates the case of a dielectric slab periodically drilled with 364 circular air holes. The sides of this finite slab are defined by $x = \pm 13.944$ and $y = \pm 2.6996$ (see Fig. 11). The permittivity of the slab is $n_i^2 = 12$, the radius of the holes is 0.294, and they are placed with hexagonal symmetry. The distance between the centers of two neighbour holes is equal to 0.68. These parameters are chosen in order to exhibit a negative refraction in *s* polarization at the wavelength $\lambda_0 = 2.02$. The structure lies in vacuum, and is illuminated by a Gaussian beam coming from the top with an incidence $\theta_0 = 30°$. The exact definition of this incident field is:

$$u^{inc}(x,y) = \int_{-\infty}^{+\infty} A(\alpha) \exp\left(\mathrm{i}\alpha x - \mathrm{i}\beta(\alpha) y\right) \mathrm{d}\alpha, \qquad (20)$$

with $\beta(\alpha)^2 = k_0{}^2 - \alpha^2$, and with a Gaussian amplitude:

$$A(\alpha) = \frac{W}{2\sqrt{\pi}} \exp\left(-\frac{(\alpha - \alpha_0)^2 W^2}{4} \right) . \qquad (21)$$

The mean incidence $\theta_0 = 30°$ of the beam is such that $\alpha_0 = k_0 \sin\theta_0$. The parameter W appearing in (21) is directly linked to the incident beam width, and is equal to $W = 5$. Figure 11 shows the resulting field map, and the negative refraction inside the crystal.

Conclusion

We have presented a method that combines the advantages of the MFS and the SMM for the study of scatterers with arbitrary shape and containing arbitrary inclusions. Note that the MFS by itself could also deal with such problems, since it is not limited to the diffraction by one homogeneous body (the extension of the MFS to several bodies is straightforward). But in many cases, the method presented here is more efficient, and particularly when the inclusions have circular cross-sections, since in that case the SMM is particularly efficient.

It is also important to note that any method able to compute efficiently the field and its derivatives inside $\mathscr{C}_0$ in the presence of sources placed outside $\mathscr{C}_0$ (problem summarized in Fig. 8) could be used in place of the SMM. In other words, the MFS could be combined with various other methods using the basic ideas described in this paper.

Let us also stress on the fact that, since the method described in this paper is based on quite intuitive foundations which remain true for three-dimensional problems, it can also be easily extended to these class of problems. For instance, the method could be useful for the study of problems dealing with a few numbers of buried objects.

Our short-term goal is to apply the method to the study of slabs made with two-dimensional photonic crystals, and in particular for the study of the negative refraction that can be observed in such structures.

References

1. D. Felbacq, G. Tayeb, and D. Maystre, "Scattering by a random set of parallel cylinders," J. Opt. Soc. Am. A 11, 2526-2538 (1994).
2. D. Felbacq, E. Centeno, "Theory of diffraction for 2D photonic crystals with a boundary," Optics Comm. **199**, 39-45 (2001).
3. T. P. White, B. Kuhlmey, R. C. McPhedran, D. Maystre, G. Renversez, C. Martijn de Sterke, and L.C. Botten, "Multipole method for microstructured optical fibers I: formulation," J. Opt. Soc. Am. B **19**, 2322-2330 (2002).
4. D. Maystre, M. Saillard, G. Tayeb, "Special methods of wave diffraction," in *Scattering*, P. Sabatier and E.R. Pike eds., (Academic Press, London, 2001).
5. G. Tayeb, R. Petit and M. Cadilhac, "Synthesis method applied to the problem of diffraction by gratings: the method of fictitious sources," in *Proceedings of the Intl Conf. on the Application and Theory of Periodic Structures*, J.M. Lerner and W.R. McKinney eds., Proc. SPIE **1545**, 95-105 (1991).
6. G. Tayeb, "The method of fictitious sources applied to diffraction gratings," Special issue on Generalized Multipole Techniques (GMT) of Applied Computational Electromagnetics Society Journal, vol. **9**, 90-100 (1994).
7. F. Zolla., R. Petit and M. Cadilhac, "Electromagnetic theory of diffraction by a system of parallel rods: the method of fictitious sources," J. Opt. Soc. Am. A **11**, 1087-1096 (1994).
8. F. Zolla and R. Petit, "Method of fictitious sources as applied to the electromagnetic diffraction of a plane wave by a grating in conical diffraction mounts," J. Opt. Soc. Am. A **13**, 796-802 (1996).

9. Y. Leviatan and A. Boag, "Analysis of electromagnetic scattering from dielectric cylinders using a multifilament current model," IEEE Trans. Ant. Prop., AP-**35**, 1119-1127 (1987).

10. A. Boag, Y. Leviatan and A. Boag, "Analysis of two-dimensional electromagnetic scattering from a periodic grating of cylinders using a hybrid current model," Radio Science **23**, 612-624 (1988).

11. A. Boag, Y. Leviatan and A. Boag, "Analysis of diffraction from echelette gratings, using a strip-current model," J. Opt. Soc. Am. A **6**, 543-549 (1989).

12. A. Boag, Y. Leviatan and A. Boag, "Analysis of electromagnetic scattering from doubly-periodic nonplanar surfaces using a patch-current model," IEEE Trans. Ant. Prop., AP-**41,** 732-738 (1993).

13. C. Hafner, *The Generalized Multipole Technique for Computational Electromagnetics*, (Artech House Books, Boston, 1990).

14. C. Hafner, "Multiple multipole program computation of periodic structures," J. Opt. Soc. Am. A **12**, 1057-1067 (1995).

15. V.D. Kupradze, "On the approximate solution of problems in mathematical physics," original (Russian): Uspekhi Mat. Nauk, **22**, 2, 59-107 (1967), English translation: Russian Mathematical Surveys **22**, 58-108 (1967).

16. D. Kaklamani and H. Anastassiu, "Aspects of the method of auxiliary sources (MAS) in computational electromagnetics," IEEE Ant. and Prop. Magazine **44**, No. 3, June 2002.

17. W. Press, B. Flannery, S. Teukolsky, W. Vetterling, *Numerical recipes in Fortran: the art of scientific computing*, 2nd edition, (Cambridge University Press, 1992).

18. A.A. Asatryan, K.Busch, R.C. McPhedran, L.C. Botten, C.M. de Sterke and N.A. Nicorovici, "Two-dimensional Green's function and local density of states in photonic

crystals consisting of a finite number of cylinders of infinite length," Phys. Rev. E **63**, 046612 (2001).

19. M. Abramovitz and I. Stegun, *Handbook of mathematical functions*, (Dover Publications, New York , 1970).
20. D. Maystre and M. Cadilhac, "Singularities of the continuation of the fields and validity of Rayleigh's hypothesis," J. Math. Phys. **26**, 2201–2204 (1985).
21. http://institut.fresnel.free.fr/fs_ssm/index.htm, or contact the authors.

Figure captions

Figure 1: Description of the problem.

Figure 2: The sources $S_{e,n}$ (represented by dots) radiate the fields $F_{e,n}(\mathbf{r})$ used to represent the scattered field u^{scat} in Ω_e, whereas the sources $S_{i,n}$ (represented by stars) radiate the fields $F_{i,n}(\mathbf{r})$ used to represent the total field u^{int} in Ω_i.

Figure 3: Cross-section of the cylinder and the two sets of sources. The profile is given by Eq. (10) and the values $c_{-5} = -0.1134 + i\,0.1310$, $c_{-4} = -0.0297 - i\,0.3238$, $c_{-3} = -0.4117 - i\,0.0973$, $c_{-2} = -0.1260 + i\,1.4149$, $c_{-1} = -2.3936 + i\,2.4031$, $c_0 = 0.5714 + i\,0.5000$, $c_1 = 1.5568 + i\,0.1876$, $c_2 = -0.1212 - i\,0.0197$, $c_3 = -0.8158 + i\,0.2155$, $c_4 = 0.2772 + i\,0.1039$, $c_5 = -0.1532 - i\,0.0102$

Figure 4: Scattered intensity at infinity for both polarizations.

Figure 5: Modulus of the total field in *p* polarization.

Figure 6: A set of $N_c = 3$ parallel cylinders in a medium with index n_i, in the case where the incident field is created by a line source.

Figure 7: Circle $\mathscr{D}_j$ surrounding the cylinder $\mathscr{C}_j$ and local co-ordinate system.

Figure 8: Setting of the problem in order to get the functions $F_{i,n}(\mathbf{r})$.

Figure 9: Field modulus in the same conditions as in Ref. [2]. The gray levels are chosen in order to match as closely as possible to that of Ref. [2].

Figure 10: Modulus of the total field for a scatterer with four inclusions.

Figure 11: Modulus of the total field. Above the slab, the black line shows the locus of the maximum of the Gaussian incident beam. Below the slab, it shows the locus of the

maximum of the transmitted field. Above the slab, the structure of the field is due to the interference between the incident and the reflected fields.

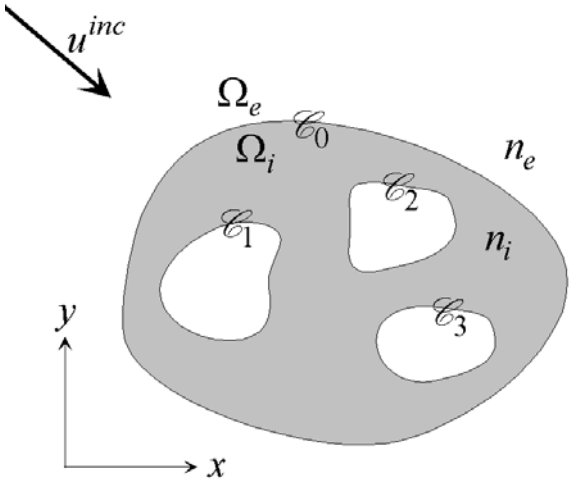

Figure 1, A-9161

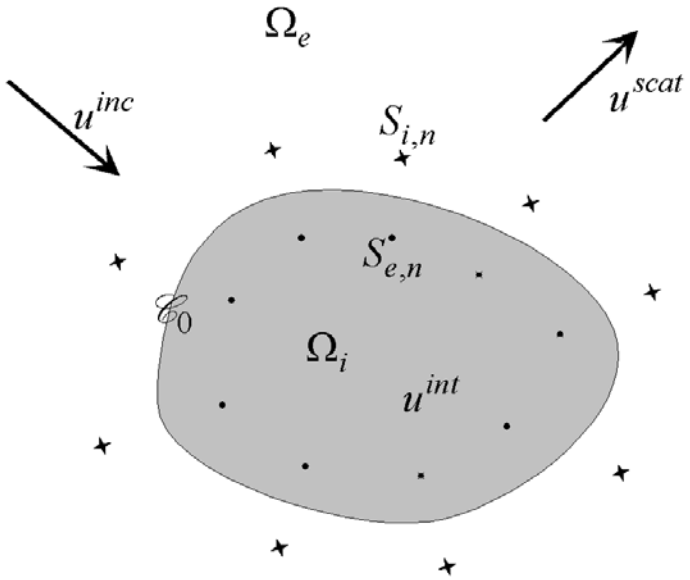

Figure 2, A-9161

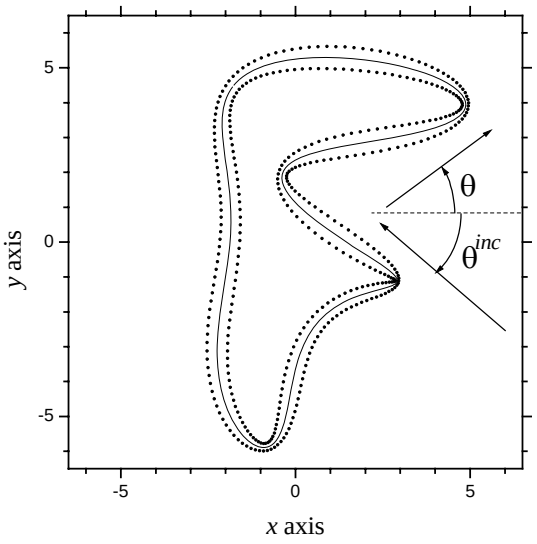

Figure 3, A-9161

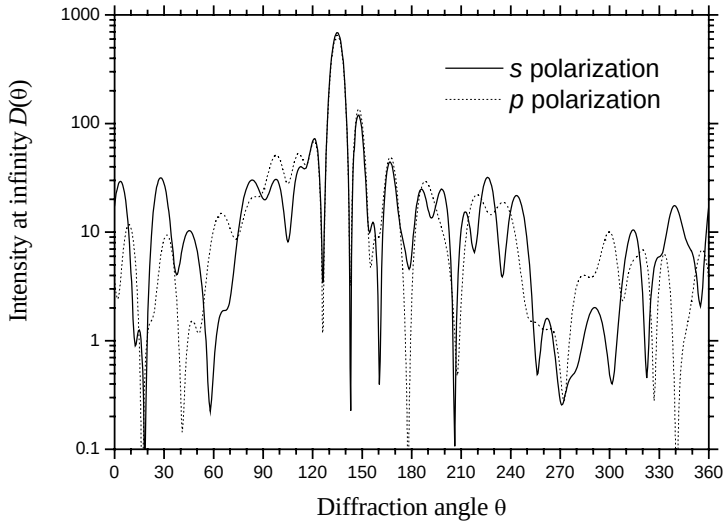

Figure 4, A-9161

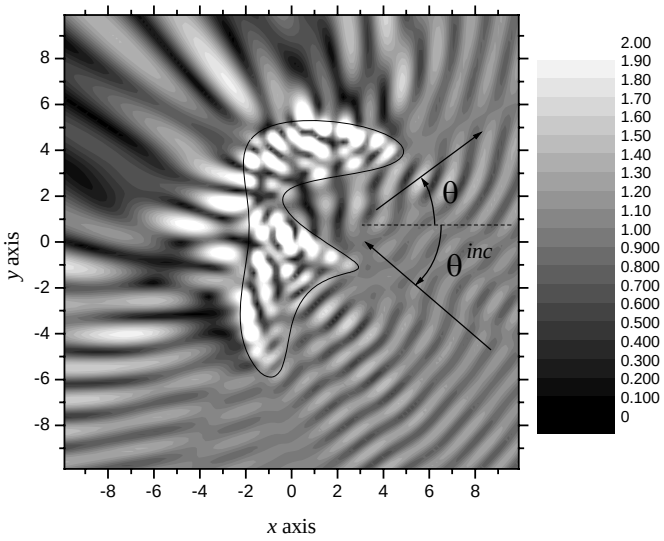

Figure 5, A-9161

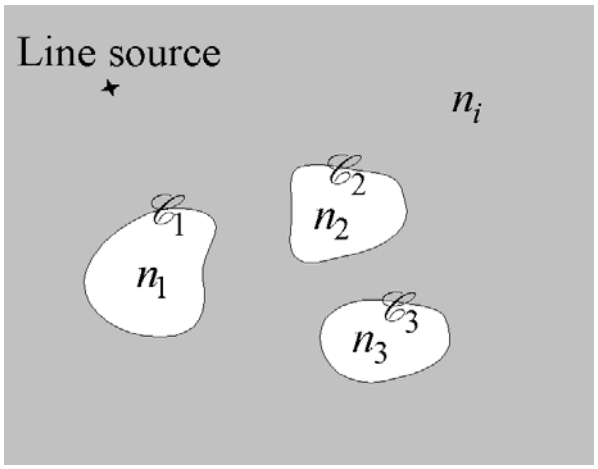

Figure 6, A-9161

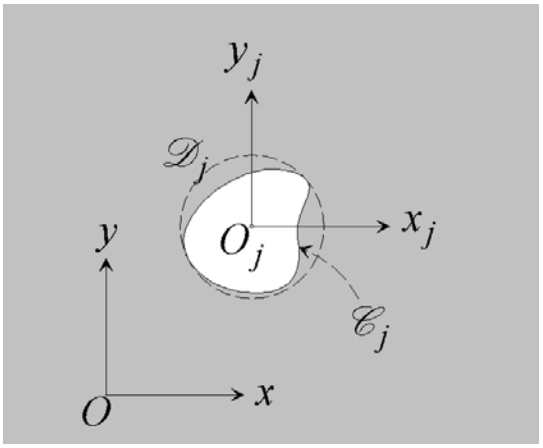

Figure 7, A-9161

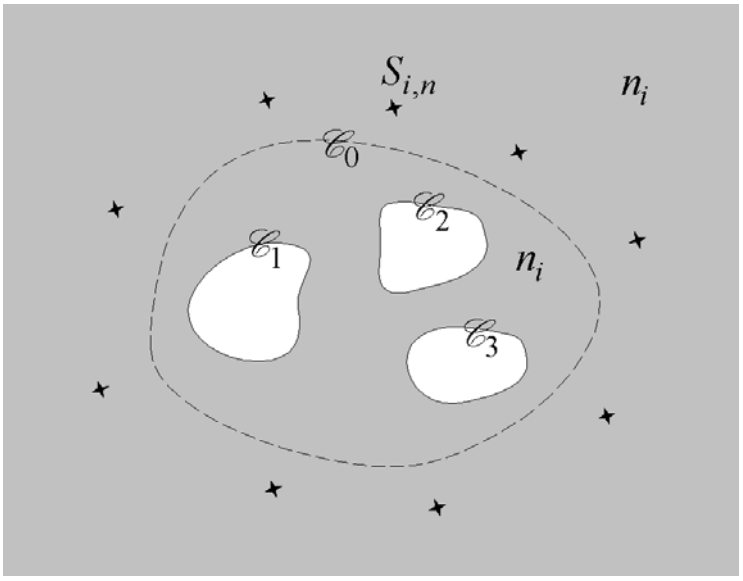

Figure 8, A-9161

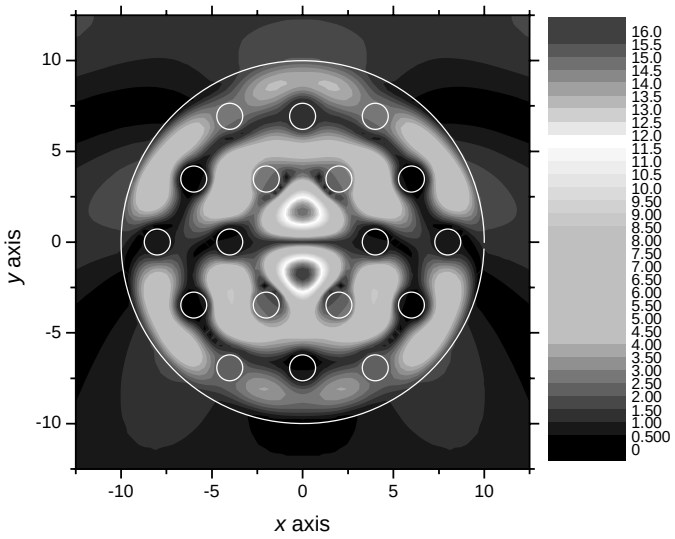

Figure 9, A-9161

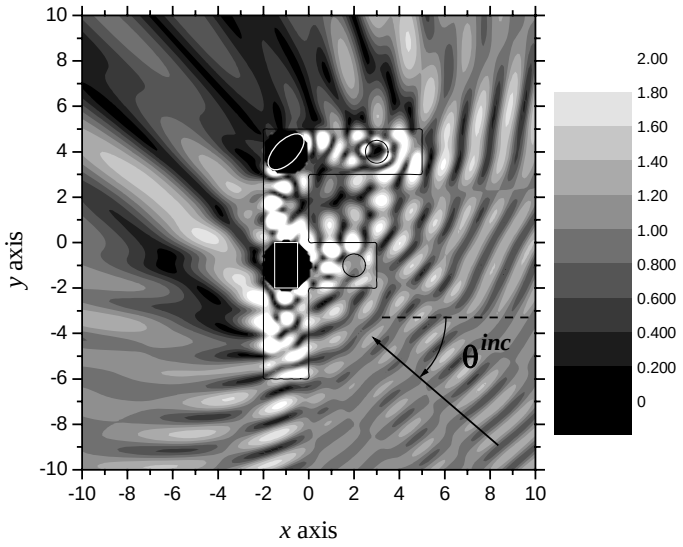

Figure 10, A-9161

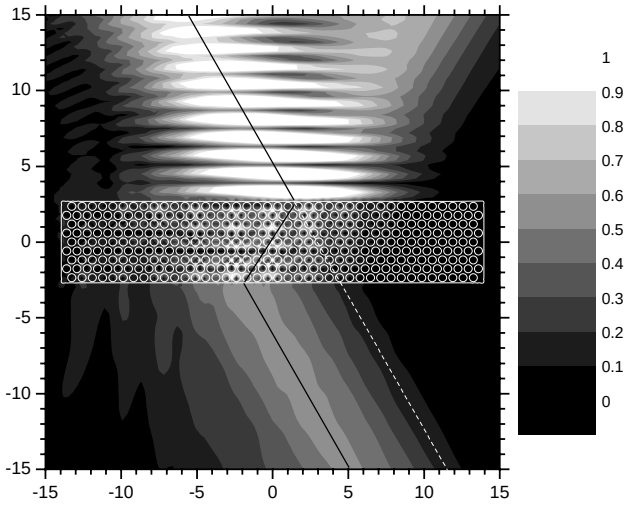

Figure 11, A-9161